

A topological approach to exploring convolutional neural networks

Yang Zhao^{a,1} and Hao Zhang^{a,1}

^aDepartment of Electric and Engineering, Tsinghua University, Beijing, China.

This manuscript was compiled on November 3, 2020

Motivated by the elusive understanding concerning convolution neural networks (CNNs) in view of topology, we present two theoretical frameworks to interpret two topics by using topological data analysis. The first one reveals the topological essence of CNN filters. Our theory first abstracts a topological representation of how the features locate for a CNN filter, named feature topology, and characterises it by defining the starting edge density. We reveal a principle of CNN filters: tending to organize the feature topologies for the same category, and thus propose the SED Distribution to statistically describe such an organization. We demonstrate the effectiveness of CNN filters reflects in the compactness of SED Distribution, and introduce filter entropy to measure it. Remarkably, the variation of filter entropy during training reveals the essence of CNN training: a filter-entropy-decrease process. Also, based on the principle, we give a metric to assess the filter performance. The second one investigates the inter-class distinguishability in a model-agnostic way. For each class, we propose the MBC Distribution, a distribution that could differentiate categories by characterising the intrinsic organization of the given category. As for multi-classes, we introduce the category distance which metricizes the distance between two categories, and moreover propose the CD Matrix that comprehensively evaluates not just the distinguishability between each two category pair but the distinguishable degree for each category. Finally, our experiment results confirm our theories.

convolution neural network | topology data analysis | clique topology | explainable AI | CNN filter

Convolutional neural networks (CNNs) have shown great power in handling dataset with gird-like topology like images. Despite non-stop explorations concerning explanations of their working mechanism, these analyses constantly bear ignorances of the underlying spatial structures in the images, leading to a continually elusive understanding. To this end, we seek to reveal two principles in a topological way: one is how CNN filters operates to the images; the other one concerns the inter-class distinguishability.

Comparing to the simplicity of convolution operation in calculation, what the CNN filters really contribute to is much more abstruse since conventional studies generally fail to specify topological information. Thus here, our work firstly concentrates on the topological representation of features looking from CNN filters, where we propose the concept of feature topology. With the successful specification of feature topology, we could further interpret how much each CNN filter contributes, and introduce the calculation of filter entropy. The filter entropy describes the organized degree of the extracted features. Significantly, it also provides another perspective to interpret the essence of training process: effective training makes the filter entropy decrease. Accordingly, we summarize our framework to finally give a metric of assessing the CNN filters. Other than current approaches, our assessment

is topology-based, and more direct and intrinsic. For example, the KSE metric, a state of the art interpretation method proposed by (2), firstly ignores the underlying spatial structures, secondly concentrates merely on the 2D kernel, thirdly interpret under requirements of strong priori knowledge and finally assess completely without considering the feature that filter tend to intrinsically extract.

As for inter-class distinguishability, given multi-categories, though a direct intuition of which category is more distinct, theoretical measure such a distinguishability is challenging especially in a model-agnostic way. Understanding the inter-class distinguishability can be fundamental in many aspects including (i) interpreting intrinsic commonalities in the same category, (ii) giving a sense of the task difficulty, (iii) instructing model selections. Unfortunately, to our knowledge, nearly no work could be found concerning this topic. Here, by unearthing the topological organizations beneath different categories, we propose a framework to theoretically evaluate the distinguishability for multi-categories. Remarkably, our framework yields a matrix, called CD Matrix, which gives a measurement of category distance between each category pair and meanwhile a degree of how distinguishable for each category.

Besides, it should be mentioned that the topological data analysis (TDA) we use here is clique topology (3). It provides an idea of mapping the locations of matrix entries to the simplicial complex, and could then yield Betti curves for a given symmetric matrix \mathbf{A} , denoting $CT(\mathbf{A}) = \beta_k(e)$, where

Significance Statement

Understanding convolutional neural networks (CNNs) is essential, but typically suffers difficulties in interpreting the special topological information. Here, we present two theoretical frameworks that separately interpret two basic topics concerning CNNs from a topological perspective. One investigates the interpretation of CNN filters, where we topologically characterize the extracted features by proposing the starting edge density; interpret the contributing degree of each filter by introducing the filter entropy; finally conclude to give a filter assessment metric. The other one theoretically analyzes the inter-class distinguishability in a model-agnostic way, and remarkably provides a distance matrix, named CD Matrix, that measures the category distance between each category pair and meanwhile quantifies the distinguishable degree for each category.

Please provide details of author contributions here.

The authors declare no conflicts of interest.

¹ A.O. (Author One) contributed equally to this work with A.T. (Author Two) (remove if not applicable).

² To whom correspondence should be addressed. E-mail: <https://www.overleaf.com/project/5efdc73f9e22220014fd46d> author.twoemail.com

$k \in \mathbb{N}_0$, β_k is the k th Betti numbers and e is the edge density.

Topological Essence of CNN Filters

Considering an image $I(x, y)$, by convolution with filters, CNN convolution layers could map the image into the feature map space,

$$F(x, y) = I(x, y) * W(x, y) \quad [1]$$

where $*$ denotes the convolution operation, $F(x, y)$ and $W(x, y)$ denote the corresponding feature map and the filter respectively. The motivation of convolution implies that large values may be expected in the feature map when local patches are similar to the convolution filters. Fig. 2A shows an illustration.

For an effective CNN filter, the existence of large values in a feature map, however, is not enough. It should satisfy both two conditions in the meantime: for each image belonged to the same category, firstly their feature map should contain large entries, which indicates the high correlation with latent features; more importantly, the locations of these large entries should shape a similar geometric structure, which indicates the inherent arrangement of the category that features should follow. The high correlation directly reflects in the values of feature maps, and we usually expect these values as high as possible. The inherent arrangement, however, instead of concerning how large the values are, concentrates on the intrinsic pattern that depend only on the locations of these large values. So for a given category, how to unveil this inherent arrangement that is abstract and fuzzy?

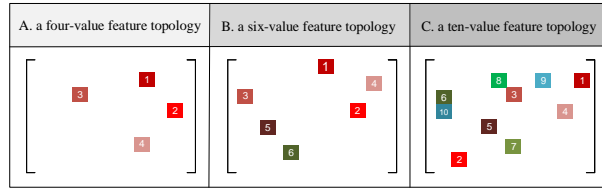


Fig. 1. An example of feature topologies where A, B and C are constructed by top four $\tau(F_1, 4)$, six $\tau(F_2, 6)$ and ten values $\tau(F_3, 10)$, respectively. In each matrix, the number on colored squared denotes the value rank of the entry.

Feature Topology. Here, we firstly introduced a concept, *feature topology*. Intuitively, for a single image, its feature topology refers to exactly the spatial arrangement of large values in the feature map, and denotes $\tau(F, v)$ where F is the feature map of the given image and v is number of top values. For example, Fig. 1 examples three different feature topologies, $\tau(F_1, 4)$, $\tau(F_2, 6)$ and $\tau(F_3, 10)$. Note that a feature topology is influenced by the number of top values we choose. Additionally, Fig. 2A marks the locations of the top ten values of the feature map in red and these ten values locate densely around the two eyes of the cat image. Remarkably, if they are randomly scattered in the feature map, it means that either the input image is not a cat or the filter is not suitable for cat category at all. Abstracting the ten values, these relative locations construct the feature topology $\tau(F, 10)$.

A feature topology is a high-level representation of how the features locate in the image. It emphasizes the relative placements of elements rather than the absolute placements,

and the orderliness rather than the values themselves. Significantly, the feature topology follows an important principle: invariant under the input transformation of shifting and rescaling, as illustrated in Fig. 2B. To reify a feature topology, we employed the method of mapping such relationship into the simplicial complex in (3). Nevertheless, different number of top values would yield different feature topologies, so we should specifically characterise the feature topology of a given image.

Starting Edge Density. For the same feature map F , the feature topologies imply a following filtration,

$$\tau(F, 1) \subset \tau(F, 2) \subset \dots \tau(F, v) \subset \dots \quad [2]$$

where the mapped simplicial complex is a single dot for $v = 1$, a line for $v = 2$, and it would become more and more complex as v increases. By calculating the Betti numbers of each mapped simplicial complex, one could obtain the Betti curves $\beta_k(v)$. Note that $\beta_k(v)$ always start from 0 and constantly keep 0 for a while, so there exists a minimum v whose $\beta_k(v)$ is non-zero. We denote this minimum v the starting edge density $S_k(F)$,

$$S_k(F) = \inf\{v | \beta_k(v) \neq 0\} \quad [3]$$

which represents the minimum number of front-rank values to construct a feature topology whose entries contain a specific "hole" topological structure, namely the minimum organized feature topology $\tau_{min}(F)$.

We believe the starting edge density is the most significant representation to characterise the feature topology of a feature map for two reasons: in the first place, it could not be influenced no matter how the smaller values are arranged; in the second place, it would not be too small, which means a sufficiency in the number of larger values that the minimum organized feature topology always contains the inherent arrangement.

SED Distribution. For an effective filter, the intrinsic arrangement of this category would tend to make each minimum organized feature topology $\tau_{min}(F)$ in the same category become similar. Here, we proposed the *SED Distribution* to describe this similarity of minimum organized feature topologies of a category in statistics. Given a category i , for image l $I_{il}(x, y)$ and its feature map $F_{il}(x, y)$, the starting edge density $S_k(F_{il}(x, y))$ could be calculated by Eq.3, and the SED Distribution is the probability distribution of the starting edge densities S_k over the entire N_i images in the category i ,

$$RV : S_k(F_{il}) \in \{0, 1, 2, \dots\}$$

$$P_{ij}(S_k(F_{il}) = x) = \frac{s_{ij}}{N_i}, \text{ where } s_{ij} = \sum_1^{N_i} \mathbb{I}_{S_k(F_{il})=x} \quad [4]$$

where $S_k(F_{il})$ and P_{ij} are separately the random variable and the probability density of the SED Distribution and s_{ij} denotes the count of the j th same starting edge density. The SED Distribution could give a direct evaluation about the filter effectiveness. The more compact in the SED Distribution, the more effective the filters are. Ideally, if the filter could always perfectly extract the target features, the starting edge densities

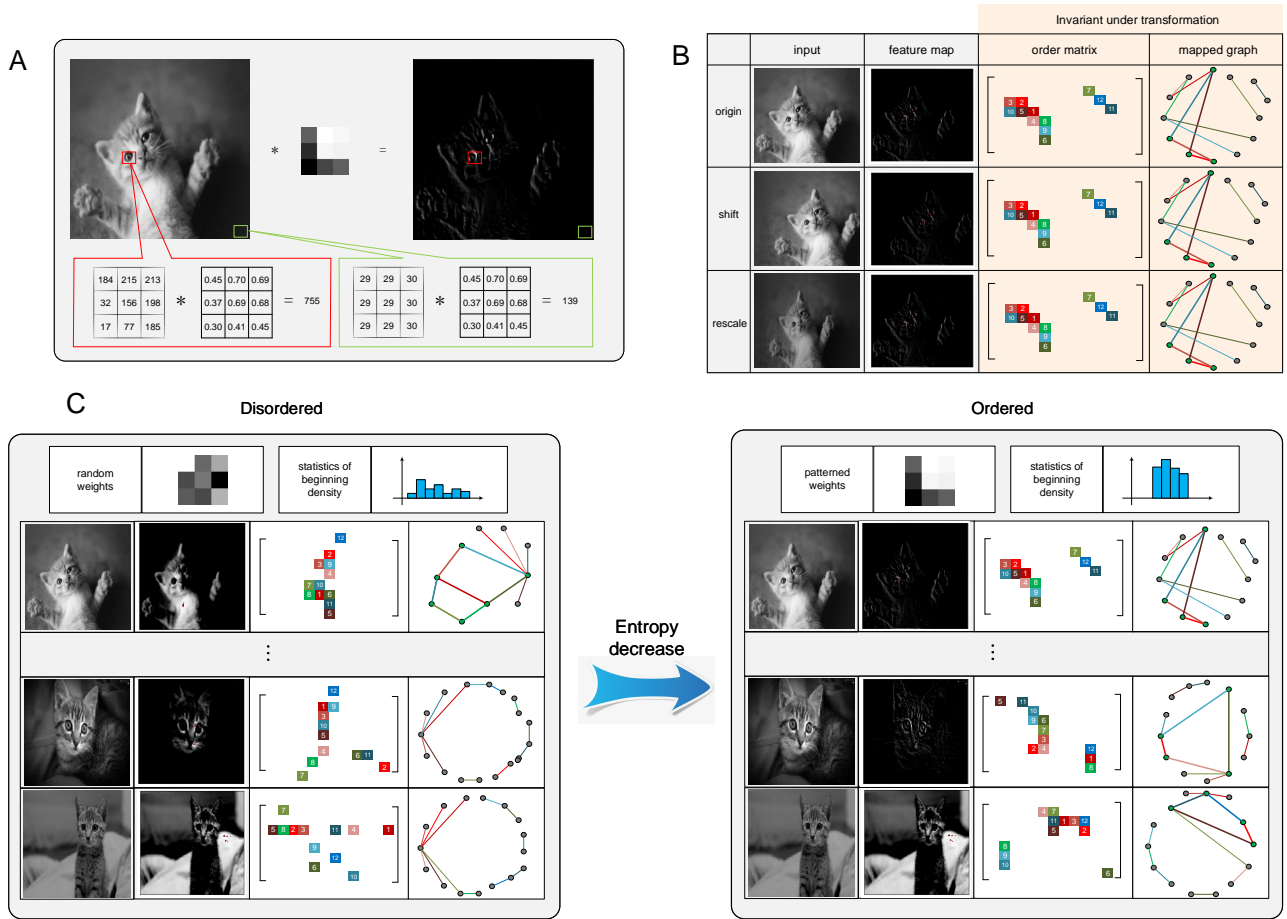


Fig. 2. CNN filter analysis using clique topology. (A) A simple example of the convolution concept: a more similar pattern with kernel would yield a larger value in feature map. Apparently, the red box is highly matched with the kernel which yields 755 after convolution, and the green box, in contrast, is 139. (B) The invariant property under transformation when using clique topology. If we shift or rescale the input image, although the values in the feature map changed, the order matrix remains the same and so does the corresponding mapped graph. This means that the topological information behind the feature map is stable under the transformation of shift or rescale. (C) The essence of CNN filters while training, which is an entropy-decrease process. For a scratched CNN, initialized with random filter weights(left), if given a class of cats, the order matrices of these feature maps present chaotic and their starting edge densities are statistically divergent, meaning a high entropy. While training, filters are learned to carry feature patterns(right). Their starting edge densities become more and more ordered and centered in statistics, and more importantly the corresponding entropy gradually decreases.

of feature maps are very likely to be the same, and the SED Distribution presents a degenerate distribution localized at the same starting edge density. On the contrary, the SED Distribution presents a discrete uniform distribution if the filter totally randomizes the feature map.

Filter Entropy. Further, in order to quantify the degree of this statistical compact, we introduced the filter entropy H of the category i ,

$$H_i = - \sum_j P_{ij} \log P_{ij} \quad [5]$$

From the entropy formula, we could easily conclude that statistical compact would yield smaller entropy than divergence. And the lower bound of this metric indicates that perfect filters could yield the smallest entropy 0, while the upper bound indicates the total chaos has the most entropy $N_i \log N_i$.

Moreover, the entropy-based evaluation implies a deeper meaning, the topological essence of training a CNN. For an

untrained CNN, filters are initialized with random parameters. Features extracted by these filters are pointless and the minimum organized feature topology $\tau_{min}(F)$ is quite chaotic. This means that for inputs in the same category, its SED Distribution is divergent in statistics and the filter entropy is high. By gradually absorbing information from datasets, training could eliminate the randomness of filters and endow these filters the ability to extract hidden features. The more effective the common feature could be extracted, the more ordered $\tau_{min}(F)$ would become. This gradual order leads to a more compact in the SED Distribution. By acquiring the dataset information, filters are trained to alleviate randomness, which directly leads to the decrease of entropy of the starting edge density.

Therefore, we could track the variation of filter entropy during training to assess the effectiveness of a filter,

$$\Delta H_i = \lim_{t \rightarrow +\infty} (H_i^{(0)} - H_i^{(t)}) \quad [6]$$

where the training process C_0, C_1, \dots, C_t is assumed fully

sufficient. If $\Delta H_i < 0$, the entropy decreases and the SED Distribution of this category gradually converges, so the filter could be considered effective for the category. On the contrary, if $\Delta H_i > 0$, the entropy increases and the filter is considered ineffective for the category.

Filter Assessment Metric. Eq.6, however, is just the assessment of the filter for a single class. We further need to assess the overall effectiveness for all classes, the ensemble filter performance. Based on the Eq.6, for each category i , we could calculate its entropy variation, and obtain an effective set \mathbb{S} that contains all the filter-entropy-decrease classes:

$$\mathbb{S} = \{i | \Delta H_i < 0, i \in \text{all classes}\} \quad [7]$$

Then, sum up all the kernel entropy of classes in the effective set:

$$E = \sum_{i \in \mathbb{S}} \Delta H_i \quad [8]$$

where E is the final assessment metric that evaluates the ensemble filter performance of all classes. Note that only decreased entropy are added in Eq.8 because we generally care less about the value that the filter entropy increases. A more disorder in the feature map does not indicate a more ineffective for the filter. Even, sometimes we may expect such a disorder in the feature map to enlarge the distance of chaos between different filters so that it could be more distinguishable for different classes.

Inter-Class Distinguishability

Inter-class distinguishability actually is the degree of to what extent could different categories be distinguished in an image classification task. For similar categories, images in each category share similar patterns, which indicates they are in similar image organizations. Quantifying this similarity, however, is very difficult especially in a model-agnostic way because conventional information evaluation could not well infuse the spatial geometric structure, such as entropy calculation based on the 1D histogram of intensities which yields no difference between a digital natural image and its random shuffle. So here, to effectively characterise the image organization, we began with introducing a concept, "constructing complexity".

Constructing Complexity. Before introducing the concept, we need to specify a kind of symmetric matrix, "geometric matrix" \mathbf{A}_g . It is constructed by sampling a set of N points in the d dimension. The matrix entries were given by $a_{ij} = \|p_i - p_j\|$, where p_i is the i th point in the sampling set. Significantly, d decides the ability of the construction. Since higher dimension can fully cover lower dimension, it will yield more various of matrices for a higher d . Due to the inner correlation between each entry, such a construction, however, could not generate matrices with random patterns no matter how high the dimension we choose.

Now consider the reverse process of this construction. Given a geometric matrix \mathbf{A}_g , the reverse of its construction exists a lower bound of the constructing dimension d_{min} , the minimum constructing dimension (MCD). If the MCD is low, the constructed points could lie in a low dimensional space and the hidden sampled points are greatly constrained. In this way, it means that the MCD measures the complexity of the

hidden sampled points in space and the effort of constructing the geometric matrix. Here, we specify such measurement the *constructing complexity*. Further, for random patterns, since no correlation would be found, a more effort of constructing it also implies a higher constructing complexity than geometric matrices. A constructing complexity is the representation of how the pixels are organized in the image, the lower the constructing complexity is, the simpler the image organization is, and the higher correlated the pixels are. Nonetheless, neither the MCD could not be acquired nor this effort could be measured directly.

Maximums of Betti Curves. Instead, we found the maximums of the Betti curves $\beta_k(e)$ could be an alternative way to measure this constructing complexity.

$$M_k(\mathbf{A}) = \max_e \beta_k(e) \quad [9]$$

which means the most "holes" that an order complex could yield.

The maximums are entirely determined by the organization of the pixels in the image, and are considered strongly influenced by the correlation between entries, the randomness in the matrix and the MCD. Notably, we found the maximums of the Betti curves could effectively quantify the constructing complexity for two reasons: firstly, a random pattern could yield a bigger maximum of the Betti curve that geometric matrices could never exceed; secondly, a bigger maximum of the Betti curve constantly denotes a higher MCD.

MBC Distribution. Similarly, we proposed the *MBC Distribution* to describe the characterisation of intrinsic organization of a category in statistic. Given a category i , for image l $I_{il}(x, y)$, the maximum of Betti curves $M_k(I_{il}(x, y))$ could be calculated by Eq.9, and the MBC Distribution is the probability distribution of the maximum of Betti curves M_k over the entire N_i images in the category i ,

$$RV : M_k(I_{il}) \in \{0, 1, 2, \dots\}$$

$$P_{ij}(M_k(I_{il}) = x) = \frac{m_{ij}}{N_i}, \text{ where } m_{ij} = \sum_1^{N_i} \mathbb{I}_{M_k(I_{il})=x} \quad [10]$$

where $M_k(I_{il})$ and P_{ij} are separately the random variable and the probability density of the MBC Distribution and m_{ij} denotes the count of the j th same maximum of Betti curves. The MBC Distribution could give the intrinsic organization of a given category a direct view. For two different categories, if their MBC Distributions are totally diverse, this indicates that none of the images in the two categories share a similar local pattern, and the pixels of each images in the two categories contain a distinct organization, so the two categories present entirely different.

Category Distance (CD). To measure the degree of similarity between the two categories, we introduced the category distance cd_{ij} between the two categories i and j ,

$$cd_{ij} = \frac{1}{2} D_{KL}(P_i \parallel R_{ij}) + \frac{1}{2} D_{KL}(P_j \parallel R_{ij}) \quad [11]$$

where $D_{KL}(\cdot)$ is the Kullback–Leibler divergence operation, P_i and P_j separately denote the MBC Distributions of the two categories, and $R_{ij} = \frac{1}{2}(P_i + P_j)$.

This formula is based on the Jensen-Shannon divergence, so the category distance has remarkable properties that it is symmetric and has a non-negative finite value. If we use the base 2 logarithm, the category distance is bounded by 1. The more closer the category distance to 1, the bigger difference these two categories are organized, and the harder to distinguish.

CD Matrix. Further, for total n categories and their MBC Distributions P_1, P_2, \dots, P_n , we define the CD Matrix \mathbf{C} as

$$\mathbf{C} = \begin{pmatrix} cd_{11} & cd_{12} & \cdots & cd_{1n} \\ cd_{12} & cd_{22} & \cdots & cd_{2n} \\ \vdots & \vdots & \ddots & \vdots \\ cd_{1n} & cd_{2n} & \cdots & cd_{nn} \end{pmatrix}_{n \times n} \quad [12]$$

where (i, j) entry is the category distance between the category i and j cd_{ij} .

Remarkably, the CD Matrix has two important properties: first, it is symmetric $\mathbf{C} = \mathbf{C}^T$, because the category distance between the i th and j th category is the same as the category distance between the j th and i th category. Also, each element on the principle diagonal is always zero, $C_{ii} = 0$, because the category distance of the i th class with itself is zero.

A CD Matrix could not just give a comprehensive view of all the CDs between each two categories, and moreover, for category i , by summing the entire column, we could quantify its distinguishable degree (DD) dd_i ,

$$dd_i = \sum_j C_{ij} \quad [13]$$

The category distance quantifies the difficulty of distinguishing the two categories, and the distinguishable degree describes which category is more distinguishable.

Experiment Results

Experiment Setup. Since our theory concentrate on the intrinsic interpretations of CNN filters and category distinguishability, it is applicable to almost any deployment concerning the two topics. So, for illustrative purposes, here we chose the image classification of handwriting digits in MNIST dataset as our experiment task, and applied the original LeNet network structure to tackle it. In the first place, such a problem is the most typical task that has been commonly studied by many researchers, so we chose it for clarity and generality. In the second place, the network is overparameterized so that our theory could be sufficiently verified because the redundancy in the model could fully categorize the images meanwhile maintain the different effectiveness of filters.

Additionally, note that the Betti curves could provide multiple dimensions (1-Betti curve, 2-Betti curve, and so on), and each Betti curve is reasonable during the whole calculation. But for higher dimensions, it would be much more difficult to yield "holes". So here, we calculated the 1-Betti curve whereas it would yield the most significant results.

Preprocessing. The prerequisite for clique topology, however, is that the input matrices should be symmetric while the images and feature maps are not. Here, we should choose a proper way to symmetrize them.

Given a feature map, for the computation of its starting edge density, considering the meaning of filters and clique topology, we should always reserve the larger entries so that the information loss is minimum during the transformation to symmetric matrices. Thus, for an $n \times n$ feature map $F(x, y)$, we proposed the following transformation,

$$F'(x, y) = \max(F, F^T) = \begin{pmatrix} a_{11} & \max(a_{12}, a_{21}) & \cdots & \max(a_{1n}, a_{n1}) \\ & a_{22} & \cdots & \max(a_{2n}, a_{n2}) \\ & & \ddots & \vdots \\ & & & a_{nn} \end{pmatrix}_{n \times n} \quad [14]$$

Given a raw image I , for the computation of its maximum of 1-Betti curve, we could simply apply the transformation of $I + I^T$ so as to get a minimum information loss.

Interpretation of CNN Filter. As our method emphasizes the convolution operation with CNN filters, it could be applied to any layer concerning this operation. To demonstrate clearly, we selected the feature maps obtained by the first convolution layer to analyze because the first convolution layer could tend to extract more general features and get more significant results(4). To investigate the variations during training, we recorded the updated model of each batch in the first epoch from the accuracy of 10% to more than 90%.

Our interpretation began with calculations of the starting edge density of each feature map by using Eq.3. Here, as an example, we randomly chose an image in class "7" and calculated the corresponding starting edge densities, $S_{1l}^{(t)}$ and $S_{1r}^{(t)}$, derived from the convolutions with two different filters at the t th iteration. The first row in Fig. 3A presents the 1-Betti curves of these feature maps, where the starting edge densities are circled in red. Notably, as the network trained, $S_{1l}^{(t)}$ gradually decreases while $S_{1r}^{(t)}$ continuously increases.

To interpret these variations, we calculated the SED Distributions of these two filters, and the second row in Fig. 3A shows the corresponding histograms. The histogram visualizes the SED Distribution, where its horizontal and vertical axes respectively stand for the values of starting edge density and the corresponding frequencies. Also, in the histograms, the red bars denote the bin that the starting edge densities $S_{1l}^{(t)}$ and $S_{1r}^{(t)}$ fall into. Clearly, as the filters updated, for the left filter, the red bars move gradually towards the centralization, and meanwhile its SED Distribution obviously presents more and more compact in the histogram. This is because training enables this filter to extract the intrinsic feature more and more effectively and the minimum organized feature topologies tend to be similar. In contrast, for the right filter, it presents totally opposite results.

Then, we calculated the filter entropy, and recorded their variations, as shown in the third row in Fig. 3A. For the left filter, the decreasing filter entropy successfully quantifies the compact variation in the SED Distribution, which we believe is effective. Significantly, to experimentally verify the filter effectiveness, we moreover investigate the variations of accuracy with and without the example filters during training process, which is shown besides the entropy decrease figure. For the left filter, if it is removed, a dramatic impact on the

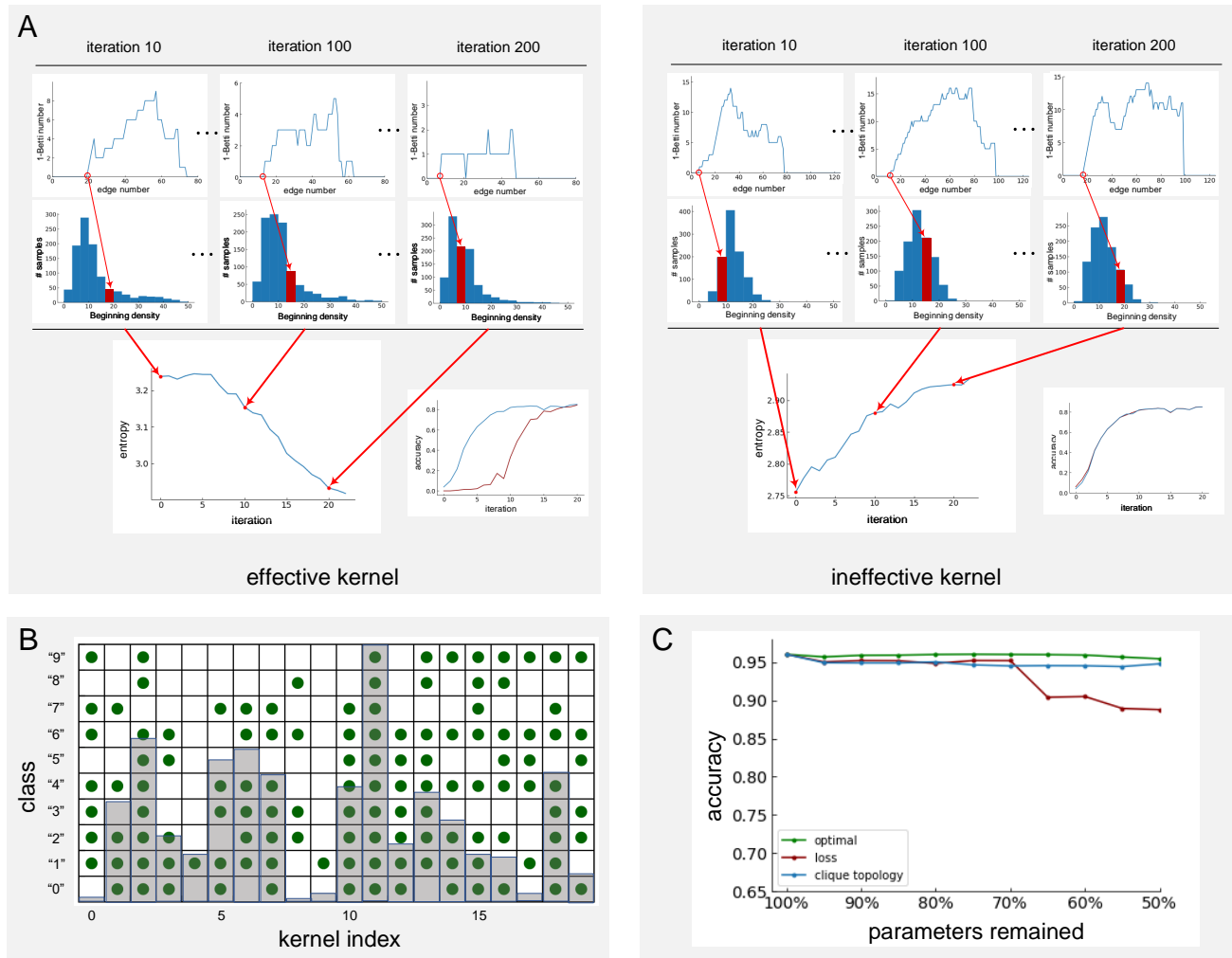


Fig. 3. Experiment results of an effective kernel(left, class "7", kernel 6) and an ineffective kernel(right, class "7", kernel 16) respectively. For the effective kernel(left), the starting edge density of the Betti curve of a feature map example moves towards smaller from 20 in iteration 1 to 8 in iteration 20, and the red bar in the histogram describes the centralized process in statistics. This results in the entropy decrease from 3.25 to about 2.92. The figure in the right bottom shows that if removing the kernel the accuracy would be badly influenced during training, which demonstrates the effectiveness of this kernel. In contrast, for the ineffective kernel(right), since the red bar in the histogram becomes deviant from center, the entropy increase from 2.75 to 2.93. And the accuracy results demonstrate nearly no influence during training when removing the kernel.

accuracy implies its effectiveness, which also validates our entropy-decrease theory.

Further, we calculated the entropy variations of each filter for each category, and by Eq.8, we could assess the ensemble performance of each filter. Fig. 3B presents the result grids, where the green dot in grid (i, j) denotes the decrease of the i th filter entropy for category j , and additionally the gray bar in each column denotes the ensemble filter entropy normalized by the maximum column value. For each row, it represents which filters could influence the category. Notably, though class "1" is influenced by most filters, one may not expect a big variation of accuracy if removing some effective filters. On the contrary, it somehow indicates class "1" is more stable comparing to other categories. As for each column, it represents the effectiveness of each filter. Note that a more green dots in the column may still yield a low ensemble entropy decrease, such as class "0" and "4".

Finally, we ranked the filters by their performance and used

it to prune the network. As an illustration, Fig. 3C shows the results that the well-trained network is pruned, and compare to the method in (1), our method outperforms the loss based method, and is very close to the optimization.

Inter-Class Distinguishability. To explore the inter-class distinguishability of the ten categories in MNIST, firstly one should calculate the maximums of 1-Betti curve for all the images and then investigate the MBC Distribution of each category. As an example, Fig. 4A shows the histograms of separately class "1", "5" and "8". Similar to the SED Distribution, the histogram gives a visualization of the MBC Distribution, where its horizontal and vertical axes respectively stand for the values of the maximum of 1-Betti curve and the corresponding frequencies. Since images in class "1" generally have a low constructing complexity, its MBC Distribution largely centers below 5. On the contrary, the values of class "5" or "8" distributes more gentle in a larger range below about 15. So, comparing the

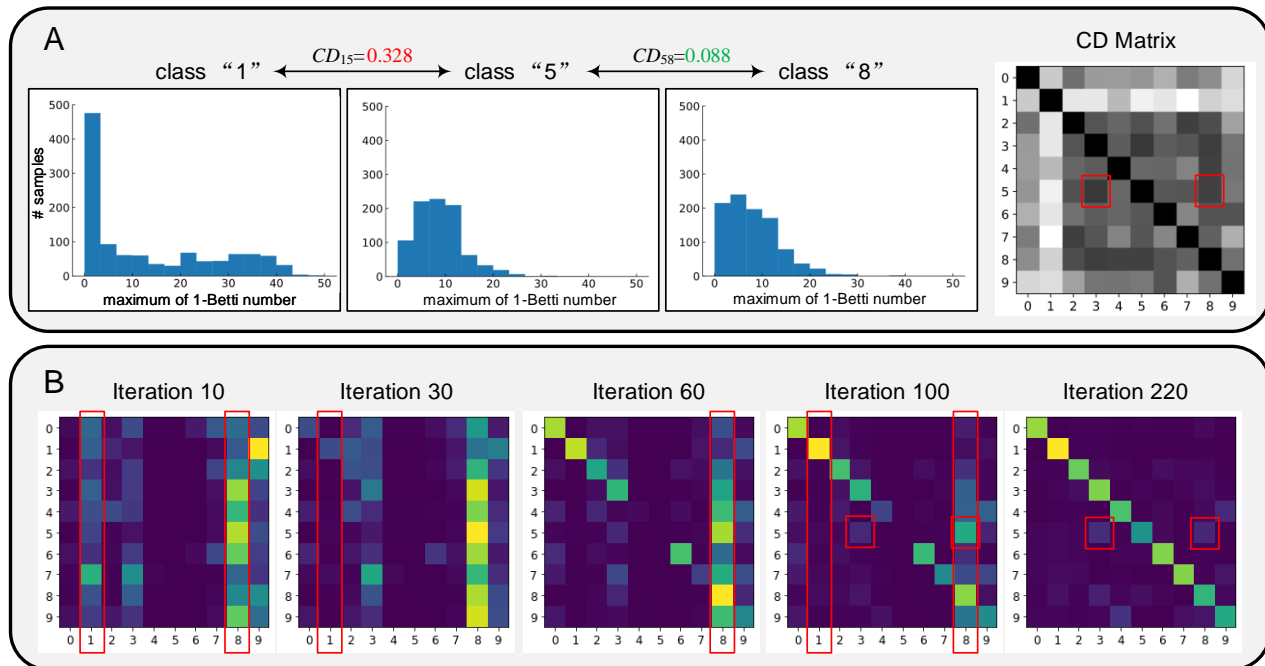


Fig. 4. Illustration of inter-class distinguishability. (A) MBC Distributions of three categories, separately class "1", "5" and "8". The distributions obviously present a much more similar between class "5" and "8" while a more different between class "1" and "5". And the following calculations of category distance shows a consistent with this point (CD_{15} is much larger than CD_{58}). Calculating each pair in the whole categories, the CD Matrix further gives a comprehensive view where the row and column denote the category pair of the category distance. Significantly, class "1" presents a most distinguishability. (B) Confusion matrices of five sequential iterations during training process. The red long boxes in the figure describe the classification status of class "1" and class "8", which indicates a strong distinguishability of class "1" and a weak distinguishability of class "8". Further, for class "5", the misclassification in the final iteration shows a consistent with the CD Matrix.

three MBC Distributions, we could easily find a much more difference between class "1" and "5" than class "5" and "8". By quantifying this difference with Eq.11, the results indicate a much larger category distance between "1" and "5" (0.328) than "5" and "8" (0.088). Undoubtedly, in our cognition, comparing to "1", "5" and "8" share more similarity, such as the "circle" in the bottom half.

Further, by calculating the category distance pairwise in the ten categories, one could acquire the CD Matrix, as shown in the right of Fig. 4A. The CD Matrix presents a clear relation of the category distance between any two categories. In the matrix, class "5" and "8" are still a tricky pair to be distinguished comparing to not only "1" and "5" but also the majority of the pairs. Additionally, by inspecting entries in each row, it gives a sense of which category could be more easily distinguished. Among the ten categories, "1" keeps relatively large category distances to all the other digits while "8" presents the opposite low category distances. Also, if applying the Eq.13, class "1" has the largest distinguishable degree, 2.73, and class "8" has the lowest distinguishable degree, 1.245. This means class "1" is the most distinguishable category while class "8" is the most confusing one.

Though the results are all very consistent with our cognition, to moreover verify our theory, we trained the network from scratch and recorded the confusion matrix of each batch in the first epoch with batch size 256. Fig. 4B sequentially gives confusion matrices of five iterations during training process. Here, two points should be noted. The first one is that the

accuracy variations of "1" and "8" with respect to the iteration obviously show a much more effort would be taken to classify class "8" than "1". The second one is that for category pair "5" and "3", "5" and "8", misclassifications between the two category pairs still partly exist at the end of this epoch, even though class "3" and "5" are not misclassified at early iteration. These two points are in an accordance with the interpretations of category distance and distinguishable degree.

Discussion

We have presented the topological interpretation of CNNs by using clique topology. Our topological interpretation consists of two parts, one is the topological essence of CNN filters, the other one is the inter-class distinguishability. Firstly, we have introduced the SED Distribution that could successfully describe the hidden structure of inputs classified to the same class. Then, we have proposed the metric, "filter entropy", to measure the performance of CNN filters, and more importantly the decrease of filter entropy reveals what training have endowed to CNN filters. Secondly, we have introduced the concept of "constructing complexity" of matrices and explored the influence on inter-class distinguishability.

Further, we have implemented an image classification experiment on the MNIST dataset. For the starting edge density, we have statistically analyzed the beginning densities of feature maps of ten categories in the dataset for each kernel in LeNet. The results show an accordance with the above entropy-decrease theory. Then, we have proposed a metric

to measure the ensemble filter performance of each kernel for all classes. And finally, the trained network is pruned according to the effectiveness ranked by the ensemble filter performance, and the pruned result outperforms the loss-based pruning method. For the maximum of Betti curve, we have explored two factors of each class, the ensemble constructing complexity and the ratio of low maximums, which strongly impact the inter-class distinguishability. Though we have empirically found the potential relation between the constructing complexity and inter-class distinguishability, the interpretation still remains in the intuitive stage and a more theoretical understanding should be presented in the future work when we gain a deeper understanding of such constructing complexity.

Finally, we would like to discuss the barriers and constraints here. Our work is analyzed using clique topology which relies heavily on the calculation of Betti curves. As the matrix dimension becomes higher, the memory and computation cost of solving such Betti curves would increase dramatically. This means it is nearly impossible to analyze matrices with large dimensions (about 140 for our server). We believe this question could be addressed by the future development of computational topology.

ACKNOWLEDGMENTS. Please include your acknowledgments here, set in a single paragraph. Please do not include any acknowledgments in the Supporting Information, or anywhere else in the manuscript.

1. P Molchanov, S Tyree, T Karras, T Aila, J Kautz, Pruning convolutional neural networks for resource efficient inference in *5th International Conference on Learning Representations*. pp. 1–17 (2017).
2. Y Li, et al., Exploiting kernel sparsity and entropy for interpretable cnn compression in *Proceedings of the IEEE Conference on Computer Vision and Pattern Recognition*. pp. 2800–2809 (2019).
3. C Giusti, E Pastalkova, C Curto, V Itskov, Clique topology reveals intrinsic geometric structure in neural correlations. *Proc. Natl. Acad. Sci.* **112**, 13455–13460 (2015).
4. J Yosinski, J Clune, Y Bengio, H Lipson, How transferable are features in deep neural networks? in *Advances in neural information processing systems*. pp. 3320–3328 (2014).